Genes and Immunity (2013) **14,** 154–161
© 2013 Macmillan Publishers Limited All rights reserved 1466-4879/13
www.nature.com/gene

ORIGINAL ARTICLE

Identification of a lupus-susceptibility locus leading to impaired clearance of apoptotic debris on New Zealand Black chromosome 13

E Pau[1,2], C Loh[1,2], GES Minty[1,2], N-H Chang[1] and JE Wither[1,2,3]

Systemic lupus erythematosus is a chronic multi-organ autoimmune disease marked mainly by the production of anti-nuclear antibodies. Nuclear antigens become accessible to the immune system following apoptosis and defective clearance of apoptotic debris has been shown in several knockout mouse models to promote lupus. However, genetic loci associated with defective clearance are not well defined in spontaneously arising lupus models. We previously showed that introgression of the chromosome 13 interval from lupus-prone New Zealand Black (NZB) mice onto a non-autoimmune B6 genetic background (B6.NZBc13) recapitulated many of the NZB autoimmune phenotypes. Here, we show that B6.NZBc13 mice have impaired clearance of apoptotic debris by peritoneal and tingible-body macrophages and have narrowed down the chromosomal interval of this defect using subcongenic mice with truncated NZB chromosome 13 intervals. This chromosomal region (81–94 Mb) is sufficient to produce polyclonal B- and T-cell activation, and expansion of dendritic cells. To fully recapitulate the autoimmune phenotypes seen in B6.NZBc13 mice, at least one additional locus located in the centromeric portion of the interval is required. Thus, we have identified a novel lupus susceptibility locus on NZB chromosome 13 that is associated with impaired clearance of apoptotic debris.

Genes and Immunity (2013) **14,** 154–161; doi:10.1038/gene.2012.64; published online 17 January 2013

Keywords: lupus; congenic mouse; macrophage clearance

INTRODUCTION

Systemic lupus erythematosus is a chronic, multi-organ autoimmune disease marked by the loss of tolerance to nuclear antigens, leading to the production of autoantibodies (autoAb) (reviewed in Kotzin[1]). The New Zealand Black (NZB) mouse spontaneously develops a lupus-like autoimmune disease similar to the human disease. Specifically, NZB mice have abnormal cellular activation and produce antibodies against nuclear antigens and red blood cells, leading to the development of glomerulonephritis and hemolytic anemia (reviewed in Theofilopoulos and Dixon[2]). Although kidney disease is mild in NZB mice, replacement of the NZB H-2^{d} MHC haplotype with an H-2^{bm12} haplotype results in severe nephritis, suggesting that the NZB background bears a full complement of non-MHC lupus susceptibility genes.[3]

Congenic mice with homozygous NZB chromosomal intervals containing one or a small cluster of these susceptibility loci introgressed onto the non-autoimmune C57BL/6 (B6) background have been very useful in dissecting the contribution of these loci to the development of lupus (reviewed in Cheung *et al.*[4]). We previously showed that genetic loci on NZB chromosome (c) 13 were associated with many of the abnormal B-cell phenotypes in this mouse strain. Consistent with these findings, B6 congenic mice with an introgressed NZB chromosome 13 interval (B6.NZBc13(47–120 Mb); denoted as B6.NZBc13 or c13) recapitulated many of these phenotypes, including increased B-cell activation and an altered B-cell subset distribution.[5] In addition, these mice produced high levels of IgM and IgG anti-chromatin autoAb, developed mild renal disease, and demonstrated expansion of activated T cells and dendritic cells (DCs), suggesting that genetic loci on this chromosome produce a generalized immunologic abnormality sufficient to develop lupus-like autoimmunity.[5] To further characterize the nature of the immune alterations in these mice, hematopoietic chimeric mice were produced in which B6.NZBc13 bone marrow alone or a mixture of B6.NZBc13 and B6.Thy1^{a}IgH^{a} bone marrow was transferred into B6.Thy1^{a}IgH^{a} recipient mice.[6] Reconstitution of B6 mice with B6.NZBc13 bone marrow transferred most of the immunologic phenotypes characteristic of B6.NZBc13 mice including B-cell activation, DC expansion and autoAb production, indicating that bone marrow-derived populations carry the immunologic defects leading to these phenotypes. However, in mice with a mixture of B6.Thy1^{a}IgH^{a} and B6.NZBc13 bone marrow cells, both B6.Thy1^{a}IgH^{a} and B6.NZBc13 B and T cells were equivalently activated.[6] This led us to postulate that an immune defect extrinsic to these populations was contributing to development of autoimmunity in B6.NZBc13 mice.

Ineffective clearance of apoptotic debris resulting in the accumulation of dying cells is thought to be one of the initiating steps in the breach of tolerance to nuclear antigens in systemic lupus erythematosus (reviewed in Munoz *et al.*[7] and Nagata *et al.*[8]). Several knockout mouse models including *C1q*, *Dnase1*, *Mer*, *LXR*, *PPARδ* and *Mfg-e8* gene deleted mice are characterized by defective clearance of apoptotic debris by macrophages and lead to a lupus-like phenotype.[9–14] Although genetic loci associated with defective clearance of apoptotic debris have rarely been

[1]Arthritis Centre of Excellence, Division of Genetics and Development, Toronto Western Research Institute, University Health Network, Toronto, Ontario, Canada; [2]Department of Immunology, University of Toronto, Toronto, Ontario, Canada and [3]Department of Medicine, University of Toronto, Toronto, Ontario, Canada. Correspondence: Dr JE Wither, Arthritis Centre of Excellence, Division of Genetics and Development, Toronto Western Hospital, Rm 1E420, 399 Bathurst Street, Toronto, Ontario, Canada, M5T 2S8.
E-mail: jwither@uhnres.utoronto.ca
Received 28 August 2012; revised 7 December 2012; accepted 11 December 2012; published online 17 January 2013

identified in spontaneously arising lupus models, B6.NZBc13 mice share many of features observed in knockout mice with impaired clearance of apoptotic debris including: abnormal activation of T and B cells and production of anti-chromatin autoAb. This similarity raised the possibility that there is impaired macrophage clearance of apoptotic debris in B6.NZBc13 mice.

In this study, we show that the peritoneal and tingible-body macrophages (TBM) of B6.NZBc13 mice are indeed impaired in their ability to uptake apoptotic debris. We further demonstrate that the genetic locus producing this defect is localized to an 81–94 Mb interval. Using subcongenic mice with truncated NZB c13 intervals, we show that this region appears to be sufficient to produce polyclonal B- and T-cell activation, together with DC expansion. However, full reconstitution of the c13 autoimmune phenotype, including autoAb production and splenomegaly, required the presence of one or more genes localized to the centromeric region on the NZB c13 interval. Our data constitute one of the first reports to identify a susceptibility locus in a spontaneous lupus-arising model that is associated with a defect in the clearance of apoptotic debris, and provide insight into how this locus interacts with other susceptibility loci on NZB c13 to promote autoimmunity.

RESULTS

Impaired clearance of apoptotic debris by c13 peritoneal macrophages

Since c13 congenic mice have autoimmune phenotypes such as production of anti-chromatin Ab and DC expansion that are typically seen in mice with impaired clearance of apoptotic debris,[5] we examined uptake of apoptotic debris by macrophages from c13 mice. To this end, B6 apoptotic thymocytes were labeled with CMTMR and 10^7 cells were injected intraperitoneally (*i.p.*) into 8- to 12-week-old B6 or pre-autoimmune c13 mice. After 30 min, peritoneal exudate cells (PEC) were harvested, stained with the macrophage-specific Ab anti-F4/80, and the proportion of F4/80$^+$ peritoneal macrophages (PM) associated with CMTMR$^+$ apoptotic debris was determined by flow cytometry. Although the number and purity of PM isolated was similar between B6 and c13 mice (data not shown), the proportion of CMTMR$^+$ PM was reduced in c13 as compared with B6 mice (Figure 1b). To further explore the possibility that uptake of apoptotic debris by PM is impaired in c13 mice, PEC were isolated and cultured with apoptotic thymocytes *in vitro*. This eliminated possible variations in the proportion of CMTMR$^+$ cells due to differences in the number or concentration of PM between the mouse strains, as both mouse strains had similar proportions of PM within their PEC with similar patterns of staining with anti-F4/80 and anti-CD11b. For these experiments, apoptotic thymocytes were labeled with pHrodo instead of CMTMR. pHrodo is a pH-sensitive dye that increases fluorescence intensity only when cells are engulfed into the acidic environment of the lysosome.[15] Thus, any differences observed would represent differences in physiological uptake rather than association of apoptotic debris with PM. As seen *in vivo*, there was reduced uptake of apoptotic thymocytes by c13 as compared with B6 F4/80$^+$ CD11b$^+$ PM *in vitro* (Figures 1a and b). To further explore the nature of the defect in c13 mice, bone marrow was cultured in M-CSF for 6 days to expand bone marrow macrophages (BMM). The number, purity and cell surface expression of F4/80 and CD11b of the harvested BMM were similar for both B6 and c13 mice (data not shown). BMM were then cultured with pHrodo-labeled apoptotic cells, as for PM. In contrast to PM, no difference was seen in uptake of apoptotic debris between the BMM from the B6 and c13 mouse strains (Figures 1a and b).

To localize the genetic polymorphism associated with this impaired clearance, a series of subcongenic mice with smaller overlapping c13 intervals were produced (Figure 2). Interestingly, all c13 subcongenic mice demonstrated similarly reduced uptake of apoptotic debris by PM (Figure 1c), tentatively mapping this defect to the 81–94 Mb region (region c shown in Figure 2). Consistent with normal clearance of apoptotic debris by full-length c13 BMM, no differences were seen for BMM between B6 and any of the subcongenic mouse strains examined (data not shown).

Reduced clearance of apoptotic debris in the germinal centers of c13 mice

Bone marrow-derived TBM have been shown to rapidly phagocytose and clear apoptotic B cells in the germinal center (GC) and mice with defects in this process, such as *Mfg-e8*-deficient mice, develop a lupus-like autoimmune disease.[14,16] To examine whether TBM in the spontaneously developing GC of c13 mice demonstrate a similar impairment in the clearance of apoptotic debris, spleens from 6-month-old mice were stained with peanut agglutinin (PNA) to detect GC, anti-CD68 to detect TBM and terminal deoxynucleotidyl transferase dUTP nick end labeling (TUNEL) reagent to detect apoptotic bodies. As seen in our previous studies, c13 mice had increased numbers of GC per spleen as compared with B6 mice (data not shown;Wither *et al*.[5]). Similarly to the findings observed in *Mfg-e8*-deficient mice,[16] there were increased numbers of TUNEL$^+$ apoptotic bodies associated with each TBM in c13 mice and these were larger and more intact than those seen in B6 mice (Figure 3a). As shown in Figure 3a, TBM-associated apoptotic bodies demonstrated the same altered morphology in all three subcongenic strains examined, again mapping this abnormality to region c on c13. The number of TUNEL$^+$ apoptotic bodies associated with TBM was further quantified by counting the number of these bodies for each TBM in the spleen section. Significantly increased numbers of apoptotic bodies were associated with TBM in the GC of full-length c13 congenic and c13 c-e and c13c-d subcongenic mice (Figure 3b). The differences observed were not due to reduced numbers of TBM per GC in c13 mice, as the number of TBM were similar or increased in the subcongenic mice and roughly paralleled the increased GC sizes (Figures 3c and d).

Since B6 mice do not spontaneously develop autoimmunity, it was possible that the differences observed between the GC of B6 and c13 congenic mice arose from differences in the specificity of their GC reactions at 6 months. To control for this possibility, 8- to 12-week-old B6 and pre-autoimmune c13 and subcongenic mice were immunized with a T-dependent antigen, NP-CGG, in alum to induce GC formation. Spleen sections from mice killed 11 days after immunization were then analyzed as outlined in the previous section. Similar numbers of GC were present in all immunized mice and little to no GC was found in unimmunized B6 and c13 mice (data not shown). As seen in spontaneously arising GC at 6 months, more TUNEL$^+$ apoptotic bodies were associated with TBM in the GC of all c13 congenic and subcongenic mice compared with B6 control mice (Figures 4a and b). The increased number of TUNEL$^+$ bodies per TBM in the c13 mouse strains was not due to reduced numbers of CD68$^+$ TBM in the GC, since there were same number or more TBM per GC in the c13 mouse strains as compared with B6 control mice and this correlated with the average size of their GC (Figures 4c and d). Nor was this the result of an increased rate of apoptosis of GC B cells in c13 mice, as levels of active caspase-3 in these cells were similar across all mouse strains tested (Figure 4e). Taken together, our findings suggest that the TBM of all c13 congenic and subcongenic mice have a defect in clearance of apoptotic debris and that the locus associated with this defect lies within in the 81–94 Mb interval (region c) of NZB c13.

Autoimmune phenotypes in c13 subcongenic mice require at least two distinct genetic loci

To determine the role of the impaired clearance of apoptotic debris in the development of lupus in c13 mice, subcongenic mice

© 2013 Macmillan Publishers Limited

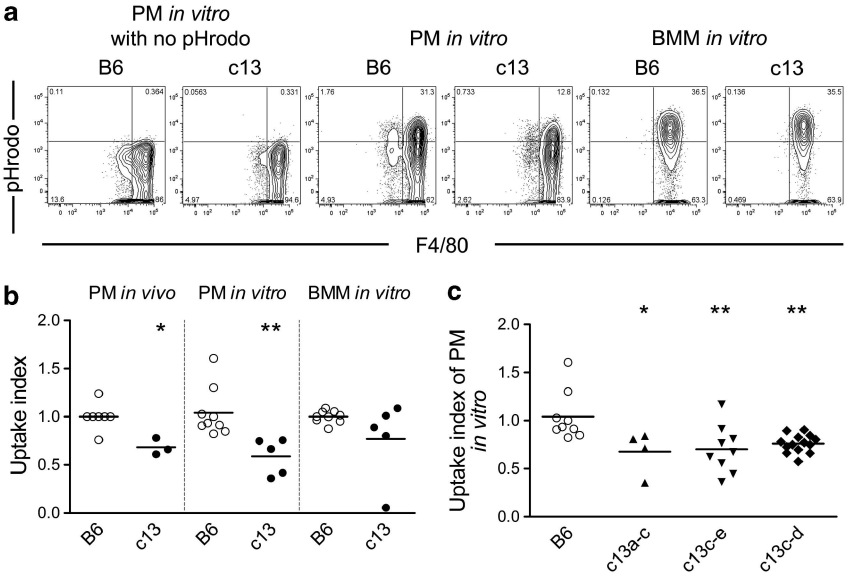

Figure 1. Impaired clearance of apoptotic debris by c13 peritoneal, but not in bone marrow-derived, macrophages *in vitro*. (**a**) Flow cytometric contour plots of B6 and c13 PM and BMM co-cultured *in vitro* with media alone (PM only), or pHrodo-labeled apoptotic cells. Plots are gated on CD11b$^+$ cells and F4/80$^+$ cells that have taken up apoptotic debris (pHrodo$^+$) are shown in the top right quadrant. (**b**) PM and BMM uptake of apoptotic thymocytes in full-length c13 mice. In all, 8- to 12-week-old B6 or pre-autoimmune c13 mice were injected *i.p.* with CMTMR-labeled apoptotic thymocytes and the PEC harvested 30 min later. Cells were stained with anti-F4/80, and the proportion of F4/80$^+$ PM that stained positively for CMTMR was determined by flow cytometry. Data are expressed as uptake index, which was defined as % CMTMR$^+$ F4/80$^+$ cells divided by the total % F4/80$^+$ cells, normalized to the mean of B6 control mice used in the same experiment. For PM and BMM *in vitro* assays, pHrodo-labeled apoptotic cells were co-incubated for 2 h with adherent PM after 2 h of resting, or BMM expanded using M-CSF for 6 days. All cells were stained with anti-F4/80 and anti-CD11b Ab before analysis by flow cytometry. The uptake index was defined as % pHrodo$^+$ CD11b$^+$ F4/80$^+$ cells divided by total % of CD11b$^+$ F4/80$^+$ cells, normalized to the mean of B6 control mice used in the same experiment. Significance levels were determined by Mann–Whitney non-parametric test: $^*P<0.05$, $^{**}P<0.005$. (**c**) Impaired uptake by PM *in vitro* was seen in all c13 subcongenic mice examined localizing the defect to region c. Experiments were performed as outlined in (**b**) on 8- to 12-week-old mice. Each symbol represents the determination from an individual mouse. Horizontal lines indicate the mean for each population examined. Significance levels were determined by one-way ANOVA with Dunns' post-test: $^*P<0.05$, $^{**}P<0.01$, $^{***}P<0.001$.

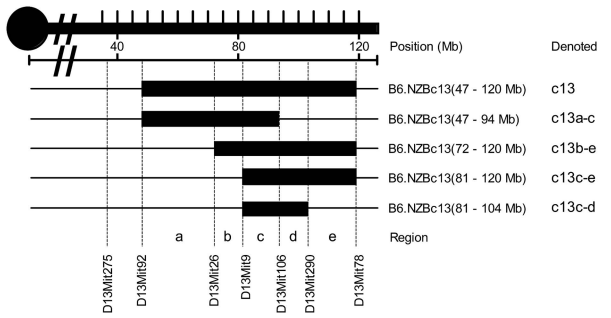

Figure 2. Genetic map of chromosome 13 subcongenic mouse strains used in the study. The subcongenic lines generated from the original B6.NZBc13(47–120 Mb) congenic mouse strain, denoted here as c13, are shown. For simplicity, the full-length c13 interval has been divided into regions (a–e) based upon the overlap between the different subcongenic mouse strains and the subcongenic strains have been renamed based upon the regions that they contain. Thick and thin black lines denote NZB and B6 regions, respectively. Polymorphic microsatellite markers used to discriminate between the B6 and NZB genome in subcongenic mice were spaced on average 4 Mb apart throughout c13 interval, and the markers used to determine the start and end markers of region are shown at the bottom of the figure. The Mb positions of the markers were determined based on Ensembl release 67 and are rounded up or down to the nearest Mb.

were aged to 6 months and their phenotypes were compared with those of age-matched B6 and c13 congenic mice. As shown in Figure 5, only the c13a-c subcongenic mouse strain produced levels of IgM and IgG anti-chromatin autoAb approaching those seen in c13 mice, with the other subcongenic strains making these autoAb to a variable extent. Notably, the c13c-d interval was not associated with significant levels of IgM or IgG anti-chromatin Ab, indicating that the apoptotic clearance defect is insufficient to produce this phenotype. This suggests the presence of a second lupus susceptibility locus in the c13 mouse strain that, based upon the similarity between full-length c13 and c13a-c mice, is most likely in region a. However, full recapitulation of the c13 phenotype may also require a locus in region b, as intermediate levels of IgG anti-chromatin Ab and increased proportions of GC B cells were seen in c13b-e mice. Nevertheless, a number of cellular phenotypes were seen in c13c-d mice, including increased expression of B-cell activation markers (Figure 5c and data not shown for B7.2 and ICAM-1), increased expression of T-cell activation markers (Figure 5e), and expansion of DC (Figure 5f). These phenotypes were also observed in c13a-c mice, localizing the genetic locus producing them to the overlapping region c containing the clearance defect. Although we have previously described expansion of the marginal zone B-cell population in the c13 mouse strain, this phenotype was not seen in the current study, possibly because of the younger age of the mice examined. However, as we had previously reported, modest increases in the splenic B1a population were seen in the c13 mice, which also localized to the c region (B6 $= 4.34 \pm 0.47$, c13a-c $= 5.89 \pm 1.10$, c13c-e $= 6.14 \pm 0.52$, mean $\pm$ s.d., $P = 0.0095$ and 0.0061, respectively). Consistent with the presence of a second susceptibility locus, splenomegaly was only seen in c13a-c mice within all the subcongenic mice (Figure 4g), which also displayed increased cellular activation and DC expansion as compared with the other subcongenic mouse strains.

© 2013 Macmillan Publishers Limited

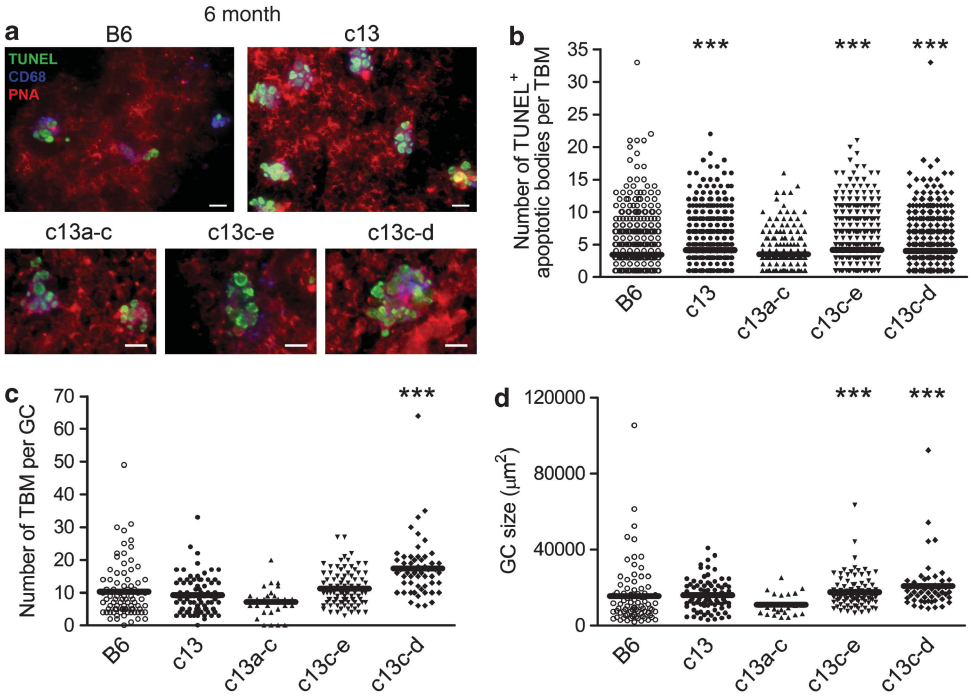

Figure 3. Increased numbers of large and more intact TUNEL$^+$ apoptotic bodies associated with spontaneously arising TBM in the GC of c13 congenic and subcongenic mice. (**a**) Apoptotic bodies, TBM and GC were visualized by TUNEL (green), anti-CD68 (blue) and PNA (red) immunofluorescent staining respectively, on 5 μm thick splenic sections of 6-month-old mice and large and intact TUNEL$^+$ bodies were seen in all c13 congenic mice. Scale bar, 10 μm. (**b**) Increased number of TUNEL$^+$ apoptotic bodies per TBM were seen in the GC of c13, c13c-e and c13c-d mice. (**c**) Number of TBM per GC and (**d**) GC size in the mouse strains examined. GC size was determined by outlining the shape of the GC in PNA-stained spleen sections using the freehand tool in Image J software. GC area was converted from px^2 to μm^2 for the respective magnification. Each symbol represents the determination from an individual GC. Number of mice used is as follows: B6, $n=9$; c13, $n=5$; c13a-c, $n=4$; c13c-e, $n=10$; c13c-d, $n=5$. Significance levels were determined by one-way ANOVA with Dunns' post-test: ***$P<0.001$.

DISCUSSION

In this study, we sought to localize lupus susceptibility loci on NZB c13 and characterize the underlying immune mechanisms that lead to the development of lupus in mice with this interval. We found that the autoimmune disease in these mice arises from at least two susceptibility loci, one of which is associated with impaired clearance of apoptotic cells by PM and TBM.

Although there are a number of reports of gene deletions that lead to reduced uptake of apoptotic debris resulting in lupus-like autoimmunity in mice, there is only one other report of a genetic region in a spontaneously arising lupus mouse model being associated with this type of defect.[17] It is unlikely that this reflects an absence of such genetic loci in these mouse models, since impaired clearance of apoptotic debris has been noted in lupus-prone MRL-*lpr*, NZB, and NZB/W mice and an abnormal response to the nuclear antigens contained in apoptotic debris is a central feature of both mouse and human lupus.[7,18,19] Instead, the difficulty in identifying these loci may result from the experimental approach that has been used to localize and characterize lupus susceptibility loci in mice. In general, these experiments have identified lupus susceptibility loci by mapping the chromosomal regions associated with autoAb production or renal disease, and then creating congenic mice with the mapped regions introgressed onto a non-autoimmune strain.[20] There is abundant evidence to suggest that these congenic intervals usually contain multiple susceptibility loci that facilitated their initial detection in mapping studies and led to the development of an autoimmune phenotype in the congenic mouse strain.[21,22] In several of the knockout mouse strains that have impaired clearance of apoptotic debris, such as *C1q* and *DNaseI* gene-deleted mice, the ability to promote lupus has been shown to be dependent upon the presence of other susceptibility loci.[9,10,23] Thus, it is probable that only those susceptibility loci associated with clearance defects in close proximity to other susceptibility loci will be found by this approach. In our study, identification of the region associated with the clearance defect was likely facilitated by the presence of a second susceptibility locus located nearby, as on its own, the region associated with the impaired clearance of apoptotic debris produces only low titer anti-chromatin Ab. Similarly, the genetic locus linking to impaired clearance that was identified in the BXSB mouse strain was found in a region of chromosome 1 that contained multiple susceptibility loci.[17] However, unlike the genetic locus reported in this study, the BXSB locus affects BMM and results in reduced uptake of antigens as well as apoptotic debris.

In c13 mice, PM and TBM, but not BMM demonstrated reduced uptake of apoptotic debris. Previous work suggests that expression of the receptors involved in the uptake of apoptotic debris differs between BMM and PM.[24–26] This differential expression may lead to functional differences between these two populations. Most notably, engulfment of apoptotic cells by PM and TBM is phosphatidylserine dependent, whereas uptake by non-activated BMM is not.[24,26] Thus, it is possible that the clearance defect in c13 mice specifically affects the phosphatidylserine-dependent pathway. In this pathway, exposure of phosphatidylserine on the surface of apoptotic cells provides an 'eat me' signal that promotes uptake of the cells by macrophages.[27] This uptake involves two stages: a first stage in which exposed phosphatidylserine on apoptotic cells binds to Tim-4 on the macrophage, resulting in adherence, and a second stage where uptake is facilitated by expression of bridging molecules that provide links between the apoptotic cells and

© 2013 Macmillan Publishers Limited

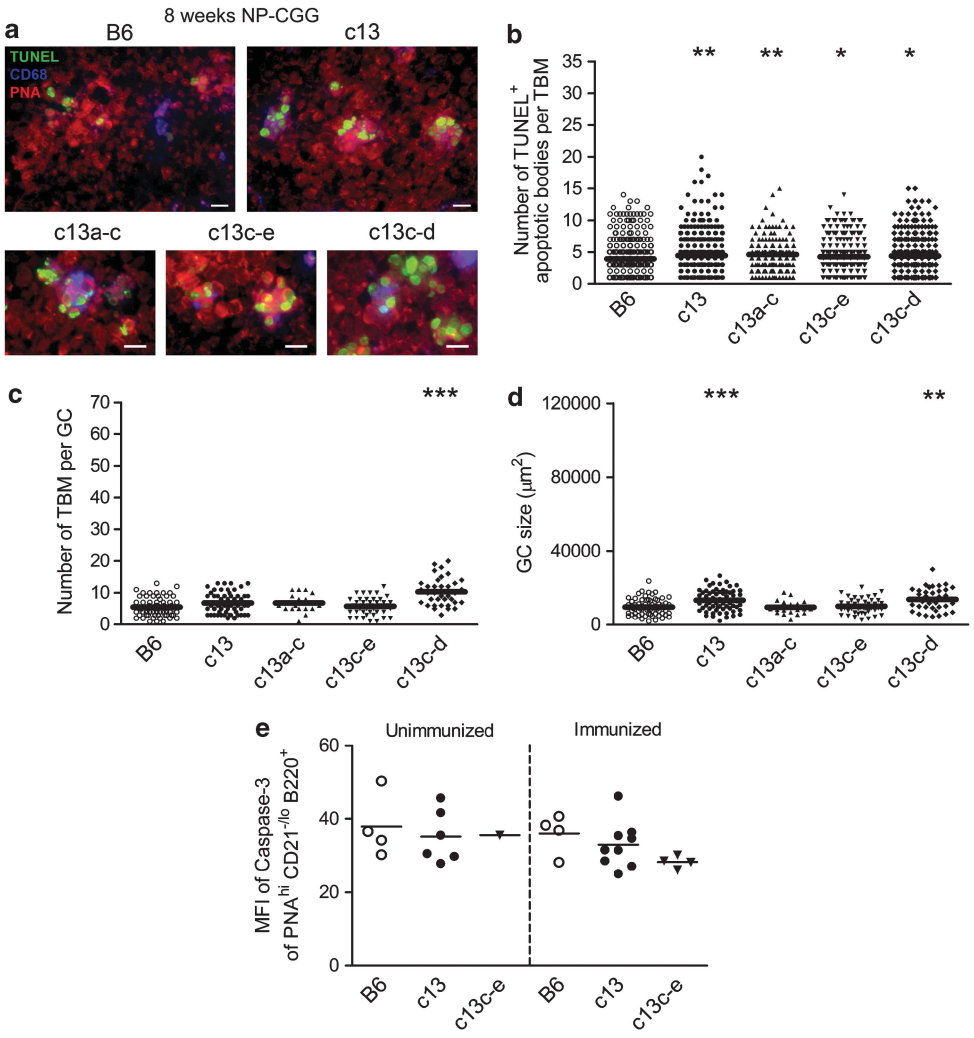

Figure 4. Impaired clearance of apoptotic debris in the germinal centers of NP-CGG immunized young c13 mice. (**a**) Apoptotic bodies, TBM and GC were visualized by TUNEL (green), anti-CD68 (blue) and PNA (red) immunofluorescent staining respectively, on 5 μm thick splenic sections of NP-CGG immunized 8- to 12-week-old mice and large and intact TUNEL$^+$ bodies were seen in all c13 congenic mice. Scale bar, 10 μm. (**b**) Increased numbers of TUNEL$^+$ apoptotic bodies per TBM were seen in the GC of all c13 congenic mice. (**c**) Number of TBM per GC and (**d**) GC size in the mouse strains examined. GC size was determined by outlining the shape of the GC in PNA-stained spleen sections using the freehand tool in Image J software. GC area was converted from px^2 to μm^2 for the respective magnification. Each symbol represents the determination from an individual GC. Number of mice used is as follows: B6, $n=12$; c13, $n=8$; c13a-c, $n=4$; c13c-e, $n=10$; c13c-d, $n=7$. (**e**) Mean fluorescent intensity (MFI) of active caspase-3 in GC B cells in the spleens of 8- to 12-week-old B6, c13 and c13c-e mice with or without NP-CGG immunization. GC B cells were gated as PNA^{hi} CD21$^{-/lo}$ B220$^+$ cells. Horizontal lines indicate the mean for each population examined. Significance levels were determined by one-way ANOVA with Dunns' post-test: $^*P<0.05$, $^{**}P<0.01$, $^{***}P<0.001$.

receptors on the macrophage. Knockout of *Tim-4* or the bridging molecules, *C1q*, or *Mfg-e8*, are associated with impaired uptake of apoptotic debris by PM and/or TBM, and have been shown to promote development of lupus.[9,14,16,28,29] While defects in either the adherence or engulfment stage of clearance by TBM can lead to increased numbers of apoptotic bodies in the GC, the close association between the increased numbers of apoptotic bodies and TBM observed in our mice suggests that the adherence stage of this process is intact. This phenotype closely mimics that seen in *Lxr* and *Mfg-e8* knockout mice, whereas in *Tim-4*-deficient mice, apoptotic bodies were mostly located adjacent to B cells.[12,16,28] We do not think that the reduced uptake of apoptotic debris by PM and TBM results from prior activation *in vivo*, as our preliminary data suggest that there are no differences in the expression of MHC class II and B7.1, or the basal levels of cytokine expression, between the resident PM of B6 and c13 mice (data not shown). Nor does this appear to arise as a consequence of the disease in c13 mice, as these changes were seen in young mice before production of autoAb and in subcongenic c13 mice that lack autoAb.

Although the clearance defect observed in our mice closely resembles that observed in *Mfg-e8* gene deleted mice, there are several important differences. *Mfg-e8* is expressed in inflammatory subsets of macrophages, such as thioglycolate-stimulated PM, and follicular DC.[16,25] *Mfg-e8* is not expressed in TBM or resident PM, the cell subsets that demonstrated impaired clearance in c13 mice. Hematopoietic chimeras showed that the *Mfg-e8* associated with TBM *in vivo* is produced by the follicular DC of the recipient mice.[16] Examination of hematopoietic chimeras where B6 or c13 bone marrow was transferred into B6 or c13 recipients indicated that transfer of the c13 bone marrow was associated with increased numbers of TBM apoptotic bodies regardless of the recipient (unpublished observations). This suggests that the defect in c13 mice may be intrinsic to TBM.

© 2013 Macmillan Publishers Limited

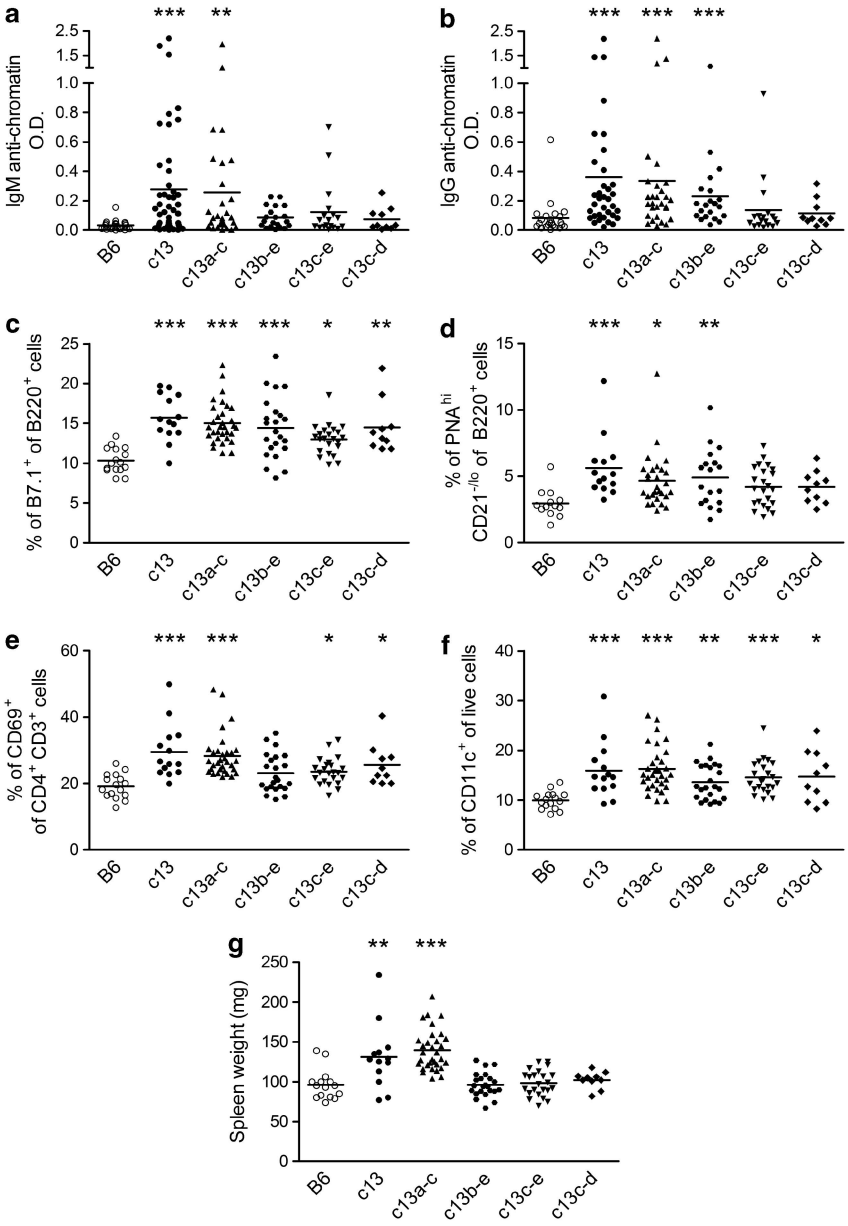

Figure 5. Autoimmune phenotypes seen in original c13 congenic mice were maintained in c13 subcongenic mouse strains. (**a**) IgM and (**b**) IgG anti-chromatin autoAb production in the serum as measured by ELISA. Increased proportions of (**c**) B7.1$^+$ B cells, (**d**) GC B cells, (**e**) CD69$^+$ CD4$^+$ CD3$^+$ T cells and (**f**) CD11c$^+$ DC cells in the spleens of c13 congenic and subcongenic mice determined by flow cytometry. (**g**) Splenomegaly was only observed in c13 congenic and c13a-c subcongenic mice. All mice used were aged to 6 months. Each symbol represents the determination from an individual mouse. Horizontal lines indicate the mean for each population examined. Significance levels were determined by one-way ANOVA with Dunns' post-test: $^*P<0.05$, $^{**}P<0.01$, $^{***}P<0.001$.

Notably, developmental endothelial locus-1 (*Del-1* or *Edil3*), a gene that is highly homologous to *Mfg-e8* in structure and function, is located in the 81–94 Mb region containing the clearance defect.[25] Evidence suggests that *Del-1* is expressed in a reciprocal fashion to *Mfg-e8*. Although there is limited data on its expression levels in primary macrophages, it has been proposed that *Del-1* is predominantly expressed in resident macrophage populations, with the exception of BMM where it is only weakly expressed. This pattern of cell expression is compatible with the cell populations that exhibit impaired clearance in c13 congenic mice, and ongoing experiments are examining this candidate gene in c13 mouse strains.

Another attractive candidate gene in the 81–94 Mb interval is autophagy-related protein 10 (*Atg10*). This is an E2-like enzyme that helps to catalyze the transfer of Atg12 to Atg5 in the initial stages of autophagosome formation (reviewed in Levine and Deretic[30]). Recently, a polymorphism in the *PRDM1-ATG5* intergenic region has been associated with systemic lupus erythematosus in a Chinese population.[31,32] Interestingly, embryos from *Atg5* knockout mice have increased amounts of apoptotic debris in their tissues.[31] Further experiments revealed that this increase resulted from impaired generation of 'eat me' and 'come and get me' signals by apoptotic cells. It is possible that Atg10 may function similarly to Atg5, affecting apoptotic cells in the GC leading to impaired uptake by TBM. However, it is unclear how this could lead to impaired clearance of B6 apoptotic cells by c13 PM, unless defective autophagy indirectly affects PM clearance function.

© 2013 Macmillan Publishers Limited

Although the 81–94 Mb interval appears to be sufficient to produce a number of the cellular abnormalities in c13 congenic mice, development of high titer autoAb production and splenomegaly requires the presence of the centromeric regions a and b, suggesting the presence of another lupus susceptibility locus. Previously, we showed that full-length c13 mice have an intrinsic B-cell defect, resulting in enhanced survival and proliferation in response to the TLR3 ligand, dsRNA analog poly(I:C).[6] We hypothesized that this defect leads to the activation nuclear antigen-reactive B cells in these mice, promoting their differentiation to autoAb-producing cells. This defect also contributed to the abnormal cellular activation and DC expansion observed in these mice, since replacement of the B-cell repertoire in c13 with an anti-hen egg white lysozyme Ig transgene resulted in significant attenuation of these phenotypes. Nevertheless, c13 Ig transgenic mice still demonstrated increases in cellular activation suggesting that another abnormality contributes to these phenotypes. Our preliminary experiments suggest that the intrinsic B-cell signaling abnormality in c13 mice is not localized to region c, and is likely located in the centromeric region of the c13 interval (unpublished observations). Thus, the immune mechanism leading to the residual activation in c13 Ig transgenic mice may be the impaired clearance of apoptotic debris, as the phenotype of these mice is similar to that seen for subcongenic mice with the c13 region c, but lacking the c13 regions a and b.

A genetic locus leading to increased serum levels of endogenous retrovirus envelope protein gp70 in NZB or NZW mice, *Sgp3* (serum gp70 production 3), has also been mapped to chromosome 13.[33] This locus has been localized to the 64.5–70 Mb interval,[34] which is located in the region in c13 interval that is associated with B-cell TLR3 hyper-responsiveness but outside the region associated with apoptotic debris clearance. It is unlikely that endogenous retrovirus is the source of dsRNA for stimulating the c13 B cells, since *Sgp3* controls the expression of gp70 from a modified polytropic ssRNA provirus.[35]

In summary, we have identified a novel lupus susceptibility locus on NZB chromosome 13 that impairs clearance of apoptotic debris. As stretches of dsRNA are found in mammalian apoptotic debris, it is likely that this clearance defect interacts directly with this B-cell defect located within the c13 to augment the autoimmune phenotype, by providing a source of endogenous TLR3 ligands. Identification of candidate genes contributing to these abnormalities will provide new understanding of the complex genetic interactions leading to the development of lupus.

MATERIALS AND METHODS

Mice

B6 mice were purchased from the Jackson Laboratory (Bar Harbor, ME, USA) and subsequently bred in our facility. The full-length NZB chromosome 13 congenic mouse strain was generated as previously described, and contains a homozygous NZB interval extending 47–120 Mb.[5] Subcongenic mice with truncated NZB chromosome 13 intervals were derived from mice with the full-length interval by backcrossing with B6 mice and selecting offspring with informative crossovers. The mice were then intercrossed to produce homozygous subcongenic mice (Figure 2). Polymorphic microsatellite markers used to discriminate the B6 and NZB genomic DNA in subcongenic mice were spaced on average 4 Mb apart throughout the c13 gene segment. All experiments were performed with 4-week to 6-month-old female mice. Mice were housed in microisolators in the animal facility at the Toronto Western Research Institute. The experiments performed in this study were approved by the Animal Care Committee of the University Health Network (Animal Use Protocol #123).

Flow cytometry

Cells were prepared for flow cytometric analysis as previously described.[5] Dead cells were excluded by staining with propidium iodide (Sigma-Aldrich, St Louis, MO, USA) at a final concentration of 0.6 $\mu g\,ml^{-1}$. Flow cytometry of stained cells was performed using FACSCalibur (Becton Dickenson; BD, Franklin Lakes, NJ, USA) and LSRII (BD) instruments and analyzed using Cell Quest Pro (BD) and FlowJo (Tree Star), respectively. The following mAbs were purchased from BD Biosciences: biotin-conjugated anti-B220 (RA3-6B2), -CD4 (L3T4), -CD11c (HL3); PE-conjugated anti-B7.1 (16-10A1), -CD69 (H1.2F3), -B220 (RA3-6B2); and FITC-conjugated anti-CD21 (7G6). Other mAbs used included biotin-conjugated anti-F4/80 (BM8; eBioscience, San Diego, CA, USA), -PNA (Sigma-Aldrich) and FITC-conjugated anti-CD11b (M1/70.15; Cedarlane Laboratories, Burlington, Ontario, Canada). Biotin staining was revealed with allophycocyanin or PerCP-conjugated streptavidin (BD). Staining for active caspase-3 was performed using the CaspGlow Fluorescein Active Caspase-3 Staining Kit (BioVision, Milpitas, CA, USA).

Measurement of Ab production

IgM and IgG anti-chromatin Abs were measured by ELISA, as described previously.[6] Bound IgM or IgG Abs were detected using alkaline phosphatase-conjugated anti-IgM or -IgG as a secondary reagent (Southern Biotech, Birmingham, AL, USA). Substrate (4-nitrophenyl phosphate disodium salt hexahydrate; Sigma-Aldrich) was added, and the OD of each well was measured at a wavelength of 405 nm.

Preparation of apoptotic cells

Thymocytes were harvested from 4- to 6-week-old B6 mice. For induction of apoptosis, RBC was removed by lysis and the remaining cells were exposed to 600 rad γ-irradiation. The cells were then cultured at 5×10^7 cells per ml in serum-free RPMI 1640 for up to 20 h at 37 °C in a humidified atmosphere of 5% CO_2, yielding $\geqslant$80% propidium iodide-positive late apoptotic thymocytes.[36] For *in vivo* uptake assays, apoptotic cells were labeled at 5×10^7 cells per ml with CellTracker Orange CMTMR (1 μM; Invitrogen, Carlsbad, CA, USA) in serum-free RPMI for 30 min at 37 °C. For *in vitro* uptake assays, apoptotic cells were labeled at 10^6 cells per ml with pHrodo succinimidyl ester (20 $ng\,ml^{-1}$; Invitrogen) in PBS for 30 min at room temperature. All labeled apoptotic cells were washed twice in PBS before resuspending in complete media (10% fetal bovine serum in RPMI-1640 containing non-essential amino acids, L-glutamine, β-mercaptoethanol, penicillin and streptomycin) for use in uptake assays.

Apoptotic cell uptake assays *in vivo* and *in vitro*

For *in vivo* uptake assays using PM, 5×10^7 CMTMR-labeled apoptotic cells in PBS were injected *i.p.* into 8- to 12-week-old mice. After 30 min, PEC were harvested from the lavage and stained with anti-F4/80. For *in vitro* uptake assays using PM, 10^6 PEC were resuspended in 1 ml complete media and rested at 37 °C for 2 h in 24-well plates. Adherent cells were washed twice in PBS before co-culturing with 4×10^6 pHrodo-labeled apoptotic cells for 2 h in complete media. For uptake assays using BMM, bone marrow cells were harvested by flushing out femurs from 8- to 12-week-old mice. Following red blood cell lysis, the cells were plated at 2×10^6 cells per ml in complete media supplemented with recombinant mouse M-CSF (10 $ng\,ml^{-1}$; R&D Systems, Minneapolis, MN, USA). Fresh media supplemented with M-CSF was replaced on day 3. On day 6, BMM were harvested using trypsin and seeded at 5×10^5 cells in 1 ml of 10% FBS/RPMI without M-CSF in 24-well plates overnight at 37 °C. The cells were then washed twice in PBS before co-culturing with 5×10^7 pHrodo-labeled apoptotic cells for 2 h. After co-culture with apoptotic cells *in vitro*, labeled apoptotic cells that were not engulfed were removed by washing with PBS, and the remaining macrophages detached from the well by scrapping. For both *in vitro* assays, all cells were stained with anti-F4/80 and -CD11b before analysis by flow cytometry. To measure the uptake of apoptotic cells by PM or BMM, an uptake index was defined as $CMTMR^+$ or $pHrodo^+$ $CD11b^+$ $F4/80^+$ cells divided by total number of $CD11b^+$ $F4/80^+$ cells, normalized to the mean of B6 control mice used in the same experiment.

Immunization

Mice at 8–12 weeks of age were immunized once *i.p.* with 200 μg of hapten 4-hydroxy-3-nitrophenyl conjugated to chicken gamma globulin (NP-CGG; Biosearch Technologies, Novato, CA, USA) precipitated in a 1:1 ratio with alum (Pierce Biotechnology, Rockford, IL, USA). Mice were killed 11 days post immunization.

Immunofluorescent staining and TUNEL analysis

Spleens were snap-frozen in Shandon Cryomatrix compound (Thermo Scientific, Rockford, IL, USA). Cryostat sections (5 μm) were fixed in 1%

© 2013 Macmillan Publishers Limited

paraformaldehyde, washed in PBS, and treated with 2:1 ratio of ethanol to acetic acid solution for 5 min at $-20\,^{\circ}C$. Slides were then blocked with 5% goat serum (Invitrogen) in PBS for 2 h, and stained with various antibodies. Purified uncongugated rat anti-mouse CD68 (FA-11; AbD Serotec, Oxford, UK) was used to detect TBM and biotin-conjugated PNA to detect GC. Goat anti-rat aminomethylcoumarin (AMCA; Jackson ImmunoResearch, Pennsylvania, PA, USA) and streptavidin rhodamine (Invitrogen) were used as secondary reagents to detect antibody staining. TUNEL assays were performed with the ApopTag Fluorescein Direct In Situ Apoptosis Detection Kit (Millipore, Billerica, MA, USA). Stained sections were mounted with Fluoro-Gel with Tris buffer (Electron Microscopy Sciences, Hatfield, PA, USA) and visualized using a Zeiss Axioplan 2 with deconvolution fluorescence microscope (Carl Zeiss, Toronto, ON, Canada). All GC from each mouse were imaged at $\times 40$ magnification, and the number of TUNEL^{+} apoptotic bodies per macrophage within the GC, total number of GC, and size of GC were counted and determined using ImageJ software (National Institutes of Health, Bethesda, MD).

Statistics

Statistical significance of comparisons between groups of mice was determined using the Mann–Whitney non-parametric two-tailed test for comparisons between two groups. For comparisons with multiple strains, statistical significance was determined by a one-way ANOVA Kruskal–Wallis test followed by Dunns' post-test for multiple comparisons. All statistical analyses were performed using GraphPad software (La Jolla, CA, USA).

CONFLICT OF INTEREST

The authors declare no conflict of interest.

ACKNOWLEDGEMENTS

This work was supported by research grants from The Arthritis Society and the Canadian Institutes of Health Research awarded to JW. JW receives salary support from The Arthritis Centre of Excellence. EP is the recipient of a studentship from the Ontario Graduate Scholarship in Science and Technology—Government of Ontario/Edward Dunlop Foundation Scholarships. CL is the recipient of a Canadian Institutes of Health Research Doctoral Research Award. GM is the recipient of a studentship from the Queen Elizabeth II/Aventis Pasteur Graduate Scholarships in Science and Technology.

REFERENCES

1 Kotzin BL. Systemic lupus erythematosus. *Cell* 1996; **85**: 303–306.
2 Theofilopoulos AN, Dixon FJ. Murine models of systemic lupus erythematosus. *Adv Immunol* 1985; **37**: 269–390.
3 Chiang BL, Bearer E, Ansari A, Dorshkind K, Gershwin ME. The BM12 mutation and autoantibodies to dsDNA in NZB.H-2bm12 mice. *J Immunol* 1990; **145**: 94–101.
4 Cheung YH, Loh C, Pau E, Kim J, Wither J. Insights into the genetic basis and immunopathogenesis of systemic lupus erythematosus from the study of mouse models. *Semin Immunol* 2009; **21**: 372–382.
5 Wither JE, Loh C, Lajoie G, Heinrichs S, Cai YC, Bonventi G *et al.* Colocalization of expansion of the splenic marginal zone population with abnormal B cell activation and autoantibody production in B6 mice with an introgressed New Zealand Black chromosome 13 interval. *J Immunol* 2005; **175**: 4309–4319.
6 Loh C, Pau E, Chang NH, Wither JE. An intrinsic B-cell defect supports autoimmunity in New Zealand black chromosome 13 congenic mice. *Eur J Immunol* 2011; **41**: 527–536.
7 Munoz LE, Lauber K, Schiller M, Manfredi AA, Herrmann M. The role of defective clearance of apoptotic cells in systemic autoimmunity. *Nat Rev Rheumatol* 2010; **6**: 280–289.
8 Nagata S, Hanayama R, Kawane K. Autoimmunity and the clearance of dead cells. *Cell* 2010; **140**: 619–630.
9 Taylor PR, Carugati A, Fadok VA, Cook HT, Andrews M, Carroll MC *et al.* A hierarchical role for classical pathway complement proteins in the clearance of apoptotic cells *in vivo*. *J Exp Med* 2000; **192**: 359–366.
10 Napirei M, Karsunky H, Zevnik B, Stephan H, Mannherz HG, Moroy T. Features of systemic lupus erythematosus in Dnase1-deficient mice. *Nat Genet* 2000; **25**: 177–181.
11 Cohen PL, Caricchio R, Abraham V, Camenisch TD, Jennette JC, Roubey RA *et al.* Delayed apoptotic cell clearance and lupus-like autoimmunity in mice lacking the c-mer membrane tyrosine kinase. *J Exp Med* 2002; **196**: 135–140.
12 A-Gonzalez N, Bensinger SJ, Hong C, Beceiro S, Bradley MN, Zelcer N *et al.* Apoptotic cells promote their own clearance and immune tolerance through activation of the nuclear receptor LXR. *Immunity* 2009; **31**: 245–258.
13 Mukundan L, Odegaard JI, Morel CR, Heredia JE, Mwangi JW, Ricardo-Gonzalez RR *et al.* PPAR-delta senses and orchestrates clearance of apoptotic cells to promote tolerance. *Nat Med* 2009; **15**: 1266–1272.
14 Hanayama R, Tanaka M, Miyasaka K, Aozasa K, Koike M, Uchiyama Y *et al.* Autoimmune disease and impaired uptake of apoptotic cells in MFG-E8-deficient mice. *Science* 2004; **304**: 1147–1150.
15 Miksa M, Komura H, Wu R, Shah KG, Wang P. A novel method to determine the engulfment of apoptotic cells by macrophages using pHrodo succinimidyl ester. *J Immunol Methods* 2009; **342**: 71–77.
16 Kranich J, Krautler NJ, Heinen E, Polymenidou M, Bridel C, Schildknecht A *et al.* Follicular dendritic cells control engulfment of apoptotic bodies by secreting Mfge8. *J Exp Med* 2008; **205**: 1293–1302.
17 Rogers NJ, Lees MJ, Gabriel L, Maniati E, Rose SJ, Potter PK *et al.* A defect in Marco expression contributes to systemic lupus erythematosus development via failure to clear apoptotic cells. *J Immunol* 2009; **182**: 1982–1990.
18 Potter PK, Cortes-Hernandez J, Quartier P, Botto M, Walport MJ. Lupus-prone mice have an abnormal response to thioglycolate and an impaired clearance of apoptotic cells. *J Immunol* 2003; **170**: 3223–3232.
19 Licht R, Dieker JW, Jacobs CW, Tax WJ, Berden JH. Decreased phagocytosis of apoptotic cells in diseased SLE mice. *J Autoimmun* 2004; **22**: 139–145.
20 Wakeland E, Morel L, Achey K, Yui M, Longmate J. Speed congenics: a classic technique in the fast lane (relatively speaking). *Immunol Today* 1997; **18**: 472–477.
21 Wakeland EK, Liu K, Graham RR, Behrens TW. Delineating the genetic basis of systemic lupus erythematosus. *Immunity* 2001; **15**: 397–408.
22 Morel L. Genetics of SLE: evidence from mouse models. *Nat Rev Rheumatol* 2010; **6**: 348–357.
23 Bygrave AE, Rose KL, Cortes-Hernandez J, Warren J, Rigby RJ, Cook HT *et al.* Spontaneous autoimmunity in 129 and C57BL/6 mice implications for autoimmunity described in gene-targeted mice. *PLoS Biol* 2004; **2**: E243.
24 Fadok VA, Laszlo DJ, Noble PW, Weinstein L, Riches DW, Henson PM. Particle digestibility is required for induction of the phosphatidylserine recognition mechanism used by murine macrophages to phagocytose apoptotic cells. *J Immunol* 1993; **151**: 4274–4285.
25 Hanayama R, Tanaka M, Miwa K, Nagata S. Expression of developmental endothelial locus-1 in a subset of macrophages for engulfment of apoptotic cells. *J Immunol* 2004; **172**: 3876–3882.
26 Miyanishi M, Tada K, Koike M, Uchiyama Y, Kitamura T, Nagata S. Identification of Tim4 as a phosphatidylserine receptor. *Nature* 2007; **450**: 435–439.
27 Ravichandran KS. Beginnings of a good apoptotic meal: the find-me and eat-me signaling pathways. *Immunity* 2011; **35**: 445–455.
28 Rodriguez-Manzanet R, Sanjuan MA, Wu HY, Quintana FJ, Xiao S, Anderson AC *et al.* T and B cell hyperactivity and autoimmunity associated with niche-specific defects in apoptotic body clearance in TIM-4-deficient mice. *Proc Natl Acad Sci USA* 2010; **107**: 8706–8711.
29 Botto M, Dell'Agnola C, Bygrave AE, Thompson EM, Cook HT, Petry F *et al.* Homozygous C1q deficiency causes glomerulonephritis associated with multiple apoptotic bodies. *Nat Genet* 1998; **19**: 56–59.
30 Levine B, Deretic V. Unveiling the roles of autophagy in innate and adaptive immunity. *Nat Rev Immunol* 2007; **7**: 767–777.
31 Qu X, Zou Z, Sun Q, Luby-Phelps K, Cheng P, Hogan RN *et al.* Autophagy gene-dependent clearance of apoptotic cells during embryonic development. *Cell* 2007; **128**: 931–946.
32 Zhou XJ, Lu XL, Lv JC, Yang HZ, Qin LX, Zhao MH *et al.* Genetic association of PRDM1-ATG5 intergenic region and autophagy with systemic lupus erythematosus in a Chinese population. *Ann Rheum Dis* 2011; **70**: 1330–1337.
33 Laporte C, Ballester B, Mary C, Izui S, Reininger L. The Sgp3 locus on mouse chromosome 13 regulates nephritogenic gp70 autoantigen expression and predisposes to autoimmunity. *J Immunol* 2003; **171**: 3872–3877.
34 Leroy V, Kihara M, Baudino L, Brighouse G, Evans LH, Izui S. Sgp3 and TLR7 stimulation differentially alter the expression profile of modified polytropic retroviruses implicated in murine systemic lupus. *J Autoimmun* 2012; **38**: 361–368.
35 Yoshinobu K, Baudino L, Santiago-Raber ML, Morito N, Dunand-Sauthier I, Morley BJ *et al.* Selective up-regulation of intact, but not defective env RNAs of endogenous modified polytropic retrovirus by the Sgp3 locus of lupus-prone mice. *J Immunol* 2009; **182**: 8094–8103.
36 Pan ZJ, Davis K, Maier S, Bachmann MP, Kim-Howard XR, Keech C *et al.* Neoepitopes are required for immunogenicity of the La/SS-B nuclear antigen in the context of late apoptotic cells. *Clin Exp Immunol* 2006; **143**: 237–248.

© 2013 Macmillan Publishers Limited